

Exploring the physicochemical processes that govern hydraulic fracture through laboratory experiments

Alpern, J. S., Marone, C. J. and Elsworth, D.

College of Earth and Mineral Sciences, The Pennsylvania State University, University Park, PA 16802

Belmonte, A.

Department of Mathematics and of Material Sciences & Engineering, The Pennsylvania State University, University Park, PA 16802

Connelly, P.

Chevron Exploration Technology Company, Houston, TX 77002

Copyright 2012 ARMA, American Rock Mechanics Association

This paper was prepared for presentation at the 46th US Rock Mechanics / Geomechanics Symposium held in Chicago, IL, USA, 24-27 June 2012.

This paper was selected for presentation at the symposium by an ARMA Technical Program Committee based on a technical and critical review of the paper by a minimum of two technical reviewers. The material, as presented, does not necessarily reflect any position of ARMA, its officers, or members. Electronic reproduction, distribution, or storage of any part of this paper for commercial purposes without the written consent of ARMA is prohibited. Permission to reproduce in print is restricted to an abstract of not more than 300 words; illustrations may not be copied. The abstract must contain conspicuous acknowledgement of where and by whom the paper was presented.

ABSTRACT: Hydrocarbon recovery is potentially maximized with an open, complex fracture network of large surface area to volume ratio that penetrates the reservoir. We study the hydraulic rupture of a solid, homogenous cube of Polymethyl methacrylate (PMMA) containing model boreholes as an analog to hydraulic fracturing with various fracture-driving fluids. The transparency of PMMA allows for the visualization of fracture propagation using high-speed video. The cubes are constrained by prescribed triaxial far-field stresses with the borehole-parallel stress set to zero. The cube is ruptured by overpressuring the borehole at controlled rates with fluids present as both liquids and gases pre- and syn- failure. We measure the fracture breakdown pressure, rates of fracture propagation and the physical characteristics of the resulting fractures and how they vary between fluid types. Further research extends these experimental methods to bluestone and granite, with additional tests that determine the permeability of these materials and its effect on creating a complex fracture network.

1. INTRODUCTION

To increase hydrocarbon recovery in the subsurface, it is desirable to produce fractures with high surface area to release the maximal amount of naturally stored oil and gas. The larger the surface area created by fractures in a finite space, the higher the potential of the system to recover hydrocarbons, because more flow channels are produced. Such a system is called an open, complex hydraulic fracture network. We investigate the creation of an open complex fracture network via laboratory experiments using a range of fracturing fluids and stress conditions. In this paper, we focus on fracture within homogenous samples, to better understand how complex networks initially develop. Once a baseline of data of fracture pressure per fluid has been made, the initial conditions can be manipulated for future experiments to create fractures of increased surface area.

2. EXPERIMENTAL PROCEDURE

Experiments were conducted in the Rock and Sediment Laboratory at the Pennsylvania State University.

2.1 Specimen and Preparation

A standard homogenous material used in hydraulic fracture experiments is Polymethyl methacrylate (PMMA) [1, 2, 3]. We used PMMA because it has known physical properties and supports stresses on order of tens of MPa, comparable to that of rock. PMMA is transparent such that fracture propagation can be analyzed during and after fracturing experiments. Here, we report results for hydraulic fracture of homogeneous cubes 101 mm (4 in) and 121 mm (5 in) on a side.

A model borehole was drilled into the PMMA cube, and set with acrylic adhesive to seal a high-pressure tube fitting and preserve the sample integrity. Boreholes were 3.66 mm (0.144 in) in diameter and tube fittings were 3.175 mm (0.125 in) in diameter. Samples were subject to biaxial and triaxial stress states, and boreholes were oriented parallel to the least principal stress direction σ_3 .

We assessed the effect of sample prestress, e.g., from casting, and borehole drilling used photoelastic images and by annealing samples after borehole installation (Figure 1). Casting prestress is clearly visible in the non-annealed sample, but comparison of hydraulic fracture characteristics for annealed and non-annealed samples showed no differences.

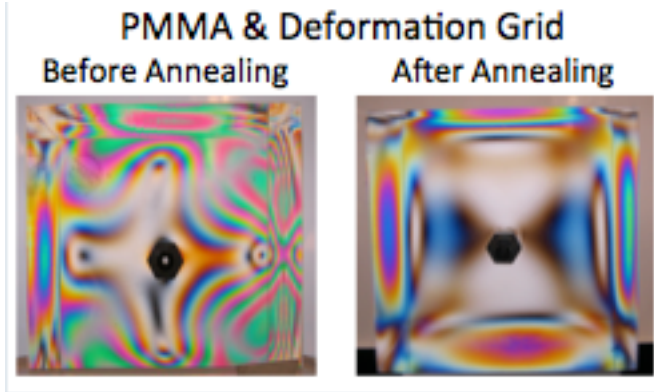


Fig. 1. PMMA cube with a deformation grid to show how the stress field changes over time. Although there is a difference in the stress fields between the annealed and un-annealed cube, this does not alter the results of the experiment.

2.2 Experimental Setup

Our tests were conducted using a servo-hydraulic, biaxial testing apparatus (Fig. 2a), fitted with independently controlled horizontal and vertical load frames [1]. We applied the horizontal load, which was

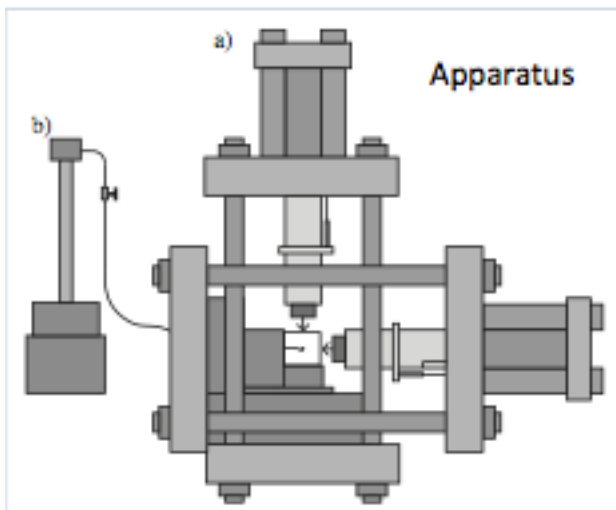


Fig. 2. Rough schematic of biaxial apparatus. Direct current displacement transducers (DCDTs) measure displacement of both hydraulic rams. Beryllium-copper load cells measure the applied force. PMMA cube is centered between the rams and attached to a pore pressure line perpendicular to the load cells.

typically the intermediate stress, σ_2 , followed by the vertical load, σ_1 [4]. For the main suite of tests reported here, the stress state was $\sigma_1 = \sigma_2 = 5$ MPa, and $\sigma_3=0$. Once the externally applied stress state was reached, we applied a pore pressure within the borehole. Pore pressure was generated using an ISCO D-series pump (Fig. 2b) with fluid at constant flow rate. Hydraulic fracturing occurred when the local borehole stresses exceeded the sample tensile strength, which is ~ 70 MPa (10,000 psi) for PMMA.

A transparent grid was attached to the cube face perpendicular to σ_3 to provide a reference frame for tracking hydraulic fracture propagation. We used a variety of visualization schemes including transmitted light with diffraction grids, for photoelastic monitoring (e.g., Fig. 1) and reflected light. Fracturing experiments were recorded with a Phantom v5.0 (*Vision Research Inc.*) high-speed digital video camera, capable of capturing up to 60,000 frames per second (fps). The camera software allows frame-by-frame examination, which we used to calculate rupture front velocity during hydraulic fracture. Our preliminary work includes only relatively crude measurements of fracture propagation velocity, because we measured rupture front position interactively, “by hand.” These estimates of rupture velocity range from 100 to 200 ms^{-1} . Future work will employ an automated method to accurately monitor rupture velocity, which is currently being developed using color recognition in MATLAB. Once this has been completed, we will conduct additional, detailed comparison of rupture velocity to assess the role of applied stress and hydraulic fracture fluid conditions.

3. RESULTS

A total of six fluids were used and include helium (He), nitrogen (N_2), carbon dioxide (CO_2), argon (Ar), sulfur hexafluoride (SF_6), and water (H_2O). These fluids were selected as they have varied properties at the temperatures and pressures used for the experiments. These physical properties of the gas include density, modulus/compressibility, viscosity, acoustic velocity thermal conductivity and heat capacity. It is anticipated that the variation of these properties between gases will influence the behavior of the fluids in driving hydraulic fractures – although the exact impact of these various properties is unknown. Apparent from the figure is that fracture pressure increases with an increase in molecular weight although the very high molecular weight Sulfur Hexafluoride appears not to conform to this trend. Initial anticipated behaviors included the expectation that (i) increased the molecular weight of the fluid may increase breakdown pressure and that (ii) increased injection rate may reduce the breakdown pressure.

3.1. Fracture Pressure

Figure 3 shows results for fracture breakdown pressure for a range of pore fluids. The complete data set shows experiments with different confining pressures in the

individual experiments is larger than any trend related to injection rate. These data also disprove our initial expectation/hypothesis that fluids of higher molecular weight will cause the PMMA to fracture at higher

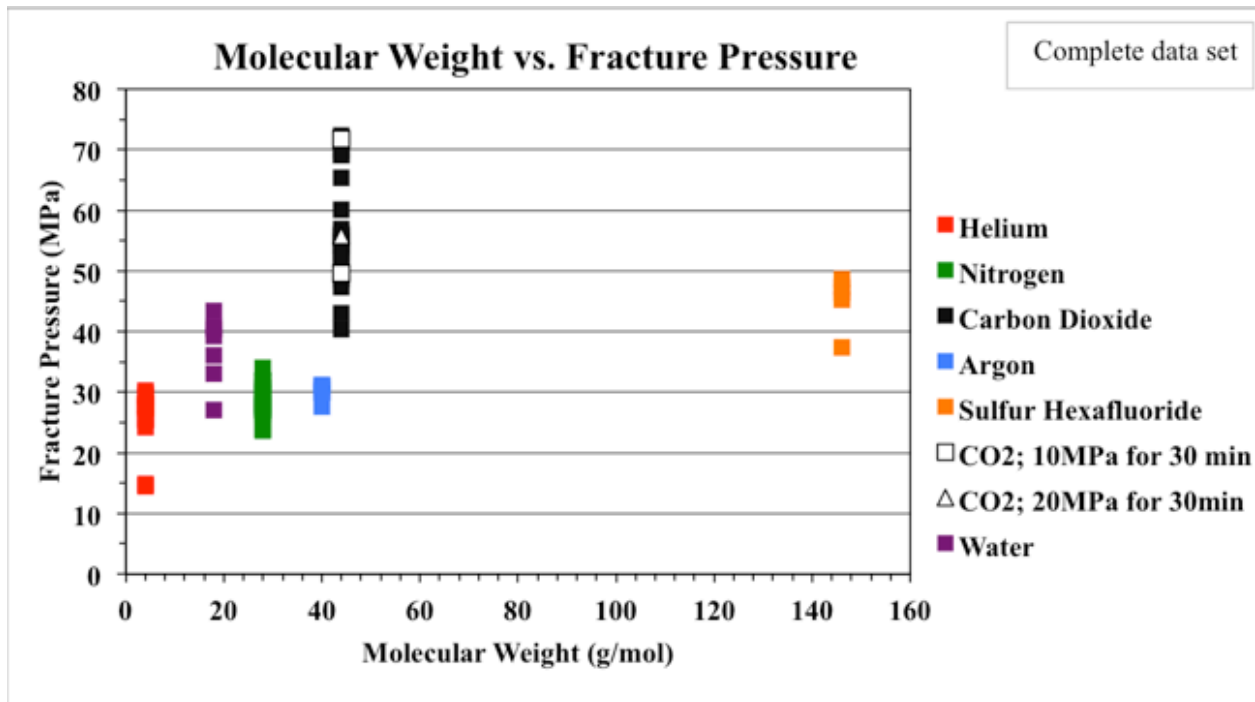


Fig. 3. Complete data set of all conducted experiments of varying initial and boundary conditions

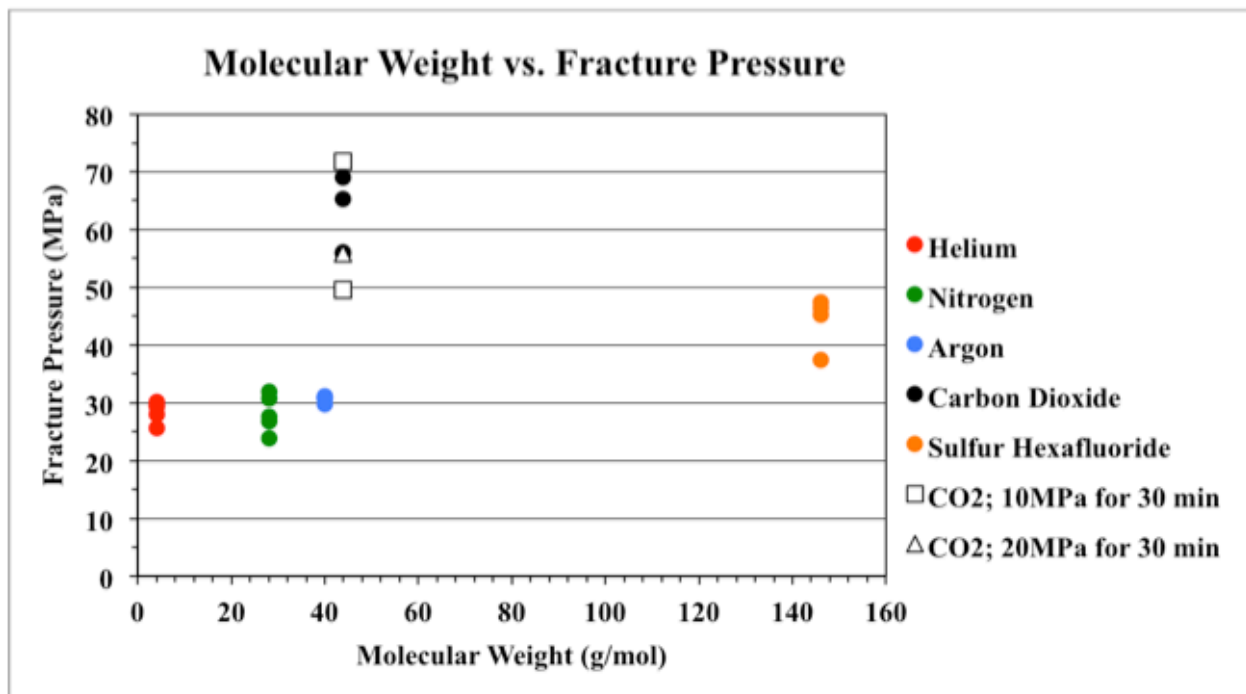


Fig. 4. Data set for experiments with the same boundary conditions. Both the vertical and horizontal confining pressures are 5 MPa.

vertical and horizontal directions and also for a variety of flow rates (Fig.3). However, even with these varying factors, there is not a significant difference between these ensemble data. Varying injection rate shows no systematic response and the variability between

pressures.

The early data for low molecular weight gases illustrate a consistent trend of fracture pressure increasing with an increase in molecular weight. However, SF₆ was

expected to fracture at pressures higher than CO₂ but fracture pressures are at the lower part of the CO₂ range. To explore the role of flow rate on fracture pressure and in attempt to lower the fracture pressure of CO₂, flow-hold- flow experiments were completed. In these, the fluid is injected at a constant flow rate until it reaches a prescribed pressure and is held at that magnitude for a set period. The pressure is then increased until rupture. However, this method was ineffective in reducing the breakdown pressure by gas infiltration or chemical weakening. This could be due to the very low permeability of PMMA [5, 6, 7].

Figure 4 shows the data for experiments with the vertical and horizontal confining pressures at uniform magnitudes of 5 MPa. Even with the restricted data set, there is still no direct relationship between molecular weight and fracture pressure (compared to Figure 3).

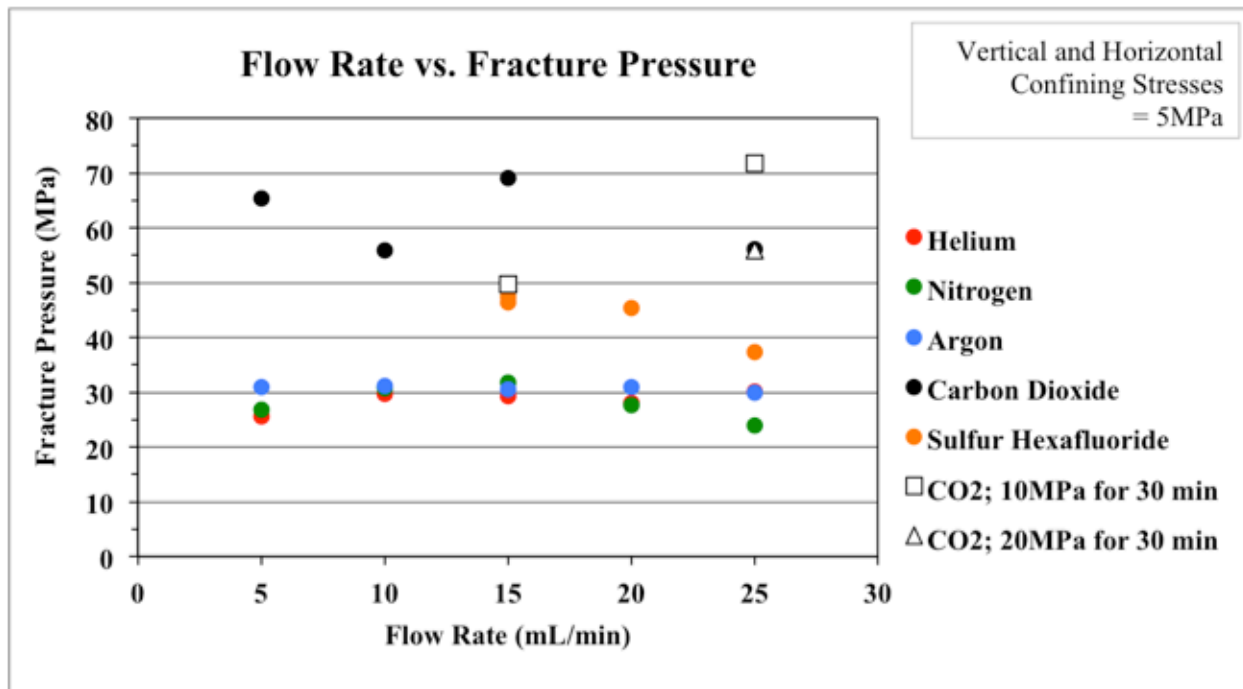


Figure 5. Data set of flow rate versus fracture pressure for experiments shown in Figure 4 with horizontal and vertical confining stresses held at 5 MPa.

The hypothesis that higher flow rates result in reduced fracture pressures was also explored by conducting experiments at multiple rates. The initial thought was a higher flow rate fills the pores quickly, causing rupture at lower pressures. Apparent from Fig. 5 is that there is no direct relationship between flow rate and fracture pressure.

3.2. Fracture Pattern

A signature fracture pattern can be associated with each fluid type. Here, we define a complex fracture pattern as one with a high surface area to volume ratio, showing an intricate fluid path through the PMMA cube [8]. This characterization is qualitative, since we cannot currently physically measure each surface area generated from

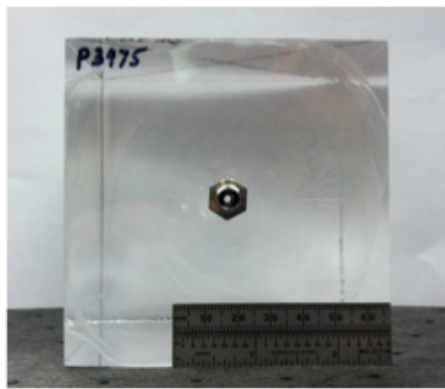
experiments. However, this result is important in establishing a network classification by providing a descriptive classification of fracture structure.

Figure 6 is the fracture resulting from PMMA fractured with carbon dioxide at 56.16 MPa at a flow rate of 25 mL/min. The fracture is simple and takes a path radially outward from the centered borehole. Figure 6(a) shows the front view of the fractured cube, and the rectangle encompasses the majority of the micro-fractures. Figure 6(b) is a side view of the same block, and shows the cube intact.

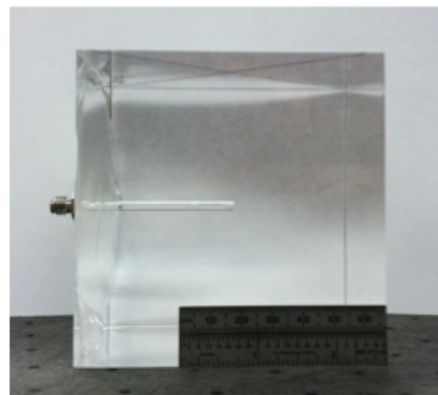
Figure 7 is the resulting fracture from an experiment where PMMA is fractured with nitrogen at 23.85 MPa and at a flow rate of 25 mL/min. The fracture is complex and helical, as a result of additional fluid entering the fracture. Figure 7(a) shows the front view of the

fractured cube with the point of fracture initiation defined. This is where the first fracture event occurred before additional gas entered the system to create the rest of the fracture. Figure 7(b) is a side view of the same block and illustrates the complexity of the fracture.

Of all the gas types, CO₂ consistently fractured as a simple fracture as did SF₆, H₂O, and He. Conversely, N₂ and Ar both consistently fractured in a complex, helical network and with the high surface area to volume ratio that was originally desired as an outcome.



(a)

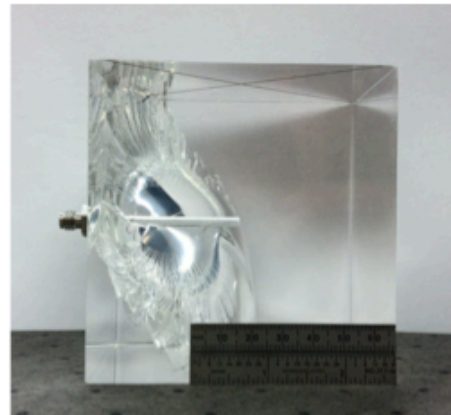


(b)

Figure 6. (a) Front view of PMMA cube fractured with carbon dioxide at 25 mL/min. Fracture is circular and simple. (b) Side view of same cube, showing the shallowness of the fracture.



(a)



(b)

Figure 7. (a) Front view of PMMA cube fractured with nitrogen gas at 25 mL/min. Fracture is helical and complex. (b) Side view of same cube, showing fracture depth and complexity.

4. DISCUSSION

Contrary to expectations from the principle of effective stress, breakdown pressures in identical block and borehole geometries and under identical stress states are shown to be dependent on fluid type. In all experiments, applied external stresses were less than 10 MPa and in the majority of experiments were of the order of a few MPa. Thus hoop stress concentrations for the maximum tensile stress are of the order of a few to ten MPa in tension. These magnitudes are small in comparison to the tensile strength of PMMA, which is of the order of 70 MPa. Therefore the breakdown pressure is principally controlled by the tensile strength of the polymer blocks being activated by the applied internal fluid pressure – allowing the results for all experiments to be considered together as in Figures 3 and 4. Regardless, the surprising effect in these experiments is the large variation in breakdown pressure that correlates with fluid type.

Breakdown pressure varies by a factor of ~3 (from ~25 MPa to ~70 MPa) for changes in the fracturing fluid, alone. In addition, there are significant changes in fracture morphology that result in a repeatable manner and consistent with the type of fracturing fluid. Future work will include applying these methods to other media; such as creating a layered sample from two cubes of PMMA sealed together, plaster of Paris, and using Green River Shale. These laboratory experiments provide an analog for the reopening of a preexisting fracture.

Similarly, since oil and gas reservoirs of our interest predominantly exist below from 1.5 to 2.5 km (about 5000 to 8000 ft) in the subsurface, where the lithostatic pressure gradient begins at 27.6 MPa (4000 psi) and increases with depth [9], future experiments will examine response at higher applied stresses.

REFERENCES

1. Anthony, J. L. and C. Marone, Influence of particle characteristics on granular friction, *J.Geophys. Res.*, 110, B08409, 10.1029/2004JB003399, 2005
2. Johnson, Edward, and Michael Cleary. "Implications of recent laboratory experimental results for hydraulic fractures." *Society of Petroleum Engineers*. 21846. (1991): 413-28.
3. Papadopoulos, Jim, V.N. Narendran, and Michael Cleary. "Laboratory Simulations of Hydraulic Fracturing." *Society of Petroleum Engineers/U.S. Department of Energy*. 11618. (1983): 161-68.
4. Elkhoury, Jean, Andre Niemejer, Emily Brodsky, and Chris Marone. "Laboratory Observations of permeability enhancement by fluid pressure oscillation of in situ fractured rock." *Journal of Geophysical Research*. 16. (2011)
5. Min, K.E., and D.R. Paul. "Effect of Tacticity on Permeation Properties of Poly(methyl methacrylate)." *Journal of Polymer Science*. 26. (1988): 1021-33.
6. Ward, I.M. *Mechanical Properties of Solid Polymers*. 2nd ed. Chinchester: John Wiley & Sons, Inc., 1983.
7. Williams, J.G. *Fracture Mechanics of Polymers*. 1st ed. Chinchester: Ellis Horwood Limited, 1984.
8. Piggott, A.R., and D. Elsworth. "Displacement of Formation Fluids by Hydraulic Fracturing." *Geotechnique*. 46.4 (1996): 671-81.
9. Karakin, A.V. "Hydraulic Fracturing in the Upper Crust." *Physics of the Solid Earth*. 42.8 (2006): 652-67.